https://doi.org/10.5194/egusphere-2026-3780
Preprint. Discussion started: 14 July 2026

Isotopic composition of aerosol iron from anthropogenic sources: implications for source apportionment of aerosol iron

Yifan Zhang[1,6,#], Guanhong Zhu[2,#], Rui Li[3], Mingyuan Liu[4], Yi Yang[5], Tianyu Zhang[1], Yizhu Chen[1], Jinlong Ma[2,*], Xinming Wang[1], Mingjin Tang[1,7,*]

[1] State Key Laboratory of Advanced Environmental Technology, Guangzhou Institute of Geochemistry, Chinese Academy of Sciences, Guangzhou, China

[2] State Key Laboratory of Deep Earth Processes and Resources, Guangzhou Institute of Geochemistry, Chinese Academy of Sciences, Guangzhou, China

[3] Department of Environmental Health, School of Public Health, Shanxi Medical University, Taiyuan, China

[4] Division of Ambient Air Monitoring, China National Environmental Monitoring Centre, Beijing, China

[5] Key Laboratory of Geographic Information Science of the Ministry of Education, School of Geographic Sciences, East China Normal University, Shanghai, China

[6] College of Earth and Planetary Sciences, University of Chinese Academy of Sciences, Beijing, China

[7] Institute of Surface-Earth System Science, School of Earth System Science, Tianjin University, Tianjin, China

[*] Correspondence: Jinlong Ma (jlma@gig.ac.cn), Mingjin Tang (mingjintang@126.com)

[#] The two authors contributed equivalently to this work.

https://doi.org/10.5194/egusphere-2026-3780
Preprint. Discussion started: 14 July 2026

Abstract

Aerosol iron (Fe) significantly impacts human health, atmospheric chemistry and marine biogeochemistry. The stable isotope ratio of Fe, typically reported as δ^{56}Fe, has emerged as a promising method for source apportionment of total and soluble aerosol Fe. However, the δ^{56}Fe endmember values remain poorly constrained for aerosol Fe from various non-dust sources, impeding the application of Fe isotopes in atmospheric research. This work measured isotopic compositions for aerosol Fe from desert dust and several anthropogenic sources. The average δ^{56}Fe was determined to be +0.14±0.10‰ for the seven dust samples we examined, in good agreement with previous work. We found that different anthropogenic aerosols exhibit a wide range of Fe isotopic composition. Compared to desert dust, the average δ^{56}Fe was found to be higher for power plant coal fly ash (+0.26±0.18‰, n=28), slightly lower for steelwork fly ash (-0.07±0.41‰, n=18), and considerably lower for biofuel burning aerosol (-0.28±0.39‰, n=11). In addition, the average δ^{56}Fe was determined to be +0.20±0.12‰ (n=2) for municipal incineration fly ash, +0.38±0.13‰ (n=1) for heavy oil bottom ash, and +0.08±0.13‰ for certificated urban particulate matter sample (n=1). We suggest that not all the anthropogenic aerosol Fe is isotopically lighter than natural dust Fe, in contrast to what is conventionally assumed. Our findings also imply that Fe isotope-based source apportionment must account for the δ^{56}Fe endmember variability both among and within different anthropogenic aerosols. Overall, our work substantially improves our ability to constrain δ^{56}Fe endmember values from various anthropogenic sources.

https://doi.org/10.5194/egusphere-2026-3780
Preprint. Discussion started: 14 July 2026

1 Introduction

Atmospheric aerosol deposition is the primary external source of dissolved iron (Fe) in the surface waters of the open ocean, influencing marine primary productivity and the global carbon cycle (Boyd and Ellwood, 2010; Moore et al., 2013; Tagliabue et al., 2017). Aerosol Fe also has important impacts on human health and atmospheric chemical processes (Zuo et al., 2022; Al-Abadleh, 2024). On the global scale, natural dust aerosol emitted from arid and semi-arid regions is the major source of total aerosol Fe (Jickells et al., 2005; Boyd et al., 2007). On the other hand, although the contribution of anthropogenic sources to total aerosol Fe is rather small, they may contribute substantially to soluble aerosol Fe as the solubility of anthropogenic aerosol Fe can be much higher than natural dust Fe (Ito et al., 2019; Rathod et al., 2020; Chen et al., 2024). Currently, it remains a great challenge to accurately distinguish and quantify the contributions of different sources to total and soluble aerosol Fe (Mahowald et al., 2018; Zhang et al., 2025).

As an emerging technique, Fe isotopes demonstrate unique advantages in source apportionment of aerosol Fe, as Fe in natural dust and anthropogenic aerosols may have distinct isotopic signatures (Fitzsimmons and Conway, 2023), typically reported as δ^{56}Fe. Natural dust aerosols from different regions exhibit relatively homogeneous Fe isotopic composition with δ^{56}Fe values around +0.1‰ (Wang et al., 2022; Wei et al., 2024; Zhang et al., 2025), being very similar to that for the upper continental crust (UCC) (Poitrasson, 2006). Field observations usually attributed lighter Fe (i.e. δ^{56}Fe lower than +0.1‰) they observed to the influence of anthropogenic emissions, and employed the two-component mixing model to quantitatively resolve the contribution of natural dust and anthropogenic sources to total and soluble aerosol Fe (Zhang et al., 2025). For instance, over the North Atlantic, the average δ^{56}Fe was found to be -1.15±0.24‰ for air masses from Europe and North America, much lower than that (+0.09±0.02‰) for air masses originating from the Saharan region (Conway et al., 2019), and

https://doi.org/10.5194/egusphere-2026-3780
Preprint. Discussion started: 14 July 2026

fossil fuel combustion was estimated to contribute 50-100% to soluble aerosol Fe observed in European and North American air masses. Another study (Kurisu et al., 2024) found δ^{56}Fe to be as low as -0.5‰ and -1.9‰ for total and soluble Fe in total suspended particles (TSP) collected over the subarctic North Pacific, and suggested that combustion contributed up to 13% and 45% of total and soluble Fe.

The δ^{56}Fe endmember values directly affect the result of Fe isotope-based source apportionment, but remain poorly constrained for anthropogenic aerosols. First, in most previous studies, a given study usually assigned a single δ^{56}Fe endmember value (usually set to the lowest δ^{56}Fe value observed) to anthropogenic aerosol Fe (Zhang et al., 2025); in other words, they did not take into account the potential difference in δ^{56}Fe endmember values for aerosol Fe from different anthropogenic sources (e.g., fossil fuel combustion, steelwork, and biomass burning). Furthermore, δ^{56}Fe endmember values adopted for anthropogenic aerosol Fe showed large variations across different studies, ranging from -4.7‰ to -1.6‰ (Conway et al., 2019; Kurisu et al., 2021; Hsieh and Ho, 2024; Kurisu et al., 2024; Bunnell et al., 2025; Shuai et al., 2025). Lastly, a few studies (Labatut et al., 2014; Bunnell et al., 2025; Camin et al., 2025) found δ^{56}Fe values significantly higher than +0.1‰ for tropospheric aerosols, and the sources and/or mechanisms which could explain the heavier Fe observed in tropospheric aerosols are still under debate.

The available measurements at present are not sufficient to provide reliable constraints on δ^{56}Fe endmember values for anthropogenic aerosols. Two recent studies (Wang et al., 2022; Wei et al., 2024) compiled aerosol Fe isotope data and then utilized the MixSIAR model to quantify aerosol Fe sources. The δ^{56}Fe endmember values adopted for anthropogenic emission display large inconsistency, for example, being -1.6±0.1‰ for fossil fuel combustion emission in one study (Wang et al., 2022), and +0.4±0.2‰ for coal combustion emission in the other study (Wei et al., 2024). As discussed in a recent review paper (Zhang et al., 2025), only a

https://doi.org/10.5194/egusphere-2026-3780
Preprint. Discussion started: 14 July 2026

limited number of studies have measured the isotopic composition of aerosol Fe from different anthropogenic sources, and these studies only examined a very small number of anthropogenic sources and a limited number of samples for each source. Moreover, the δ^{56}Fe endmember values of biomass burning aerosol, which may be an important source for soluble aerosol Fe (Mead et al., 2013; Li et al., 2025), have not been determined.

The lack of reliable δ^{56}Fe endmember values for anthropogenic aerosols limits the application of Fe isotopes in atmospheric aerosol research. This study measured the isotopic composition of aerosol Fe from several important anthropogenic emissions, including coal fly ash, steelwork fly ash, biofuel burning aerosols, municipal incineration fly ash, heavy oil bottom ash, and certificated urban particulate matter sample. In contrast to what is conventionally assumed, we found that not all the anthropogenic aerosol Fe is isotopically lighter than natural dust Fe. Moreover, large variabilities in Fe isotopic compositions were revealed among and within different anthropogenic aerosols. Our measured δ^{56}Fe endmember values can be important for quantitative isotope-based source apportionment of aerosol Fe.

2 Materials and Methods

2.1 Sample information

This study measured the Fe isotope compositions for seven types of particulate samples, consisting of desert dust, power plant coal fly ash, steelwork fly ash, biofuel burning aerosols, municipal waste fly ash, oil bottom ash, and urban particulate matter.

2.1.1 Desert dust, power plant coal fly ash, and steelwork fly ash

Seven desert dust samples were examined (Table 3), comprising Saharan dust, Arizona Test Dust (ATD, nominal 0-3 μm fraction), Luochuan loess (LC loess), Taklimakan dust (TK dust), Gobi dust (GB dust), Qinghai dust (QH dust), and Tibetan Plateau dust (Tibet dust). Saharan dust was collected at the Cape Verde Islands (Chen et al., 2020), ATD was purchased from Powder Technology, Inc., USA, and the last five dust samples were collected from

https://doi.org/10.5194/egusphere-2026-3780
Preprint. Discussion started: 14 July 2026

different regions in China.

Among the 28 power plant coal fly ash samples we studied (Table S3), 26 samples were provided by large coal-fired power plants from 25 provinces in China (Li et al., 2025), one sample was the certified reference material (GBW08401) provided by the Research Center for Eco-Environmental Sciences, Chinese Academy of Sciences (Li et al., 2022), and one sample (CFA-FDU) was provided by Fudan University (Wu et al., 2023).

The 21 steelwork fly ash samples (Table S4) were provided by large and medium-sized steelwork plants located in different regions in China (Li et al., 2025). These samples were emitted from several major steelwork processes, including coking (n=3), sintering (n=5), blast furnace (n=2), converter (n=2), post-steelmaking (n=1), and casting (n=1). Samples could be provided by the same plant or obtained from the same/similar steelwork processes, while there were no two samples obtained from the same process in the same plant. Among the 21 samples, 12 samples were collected from baghouses or electrostatic precipitators, 2 blast furnace fly ash samples were obtained from gravity settlers, and the other 7 samples were collected from chimney outlets. All the samples were dried in an oven (65 °C) for 24 hours, and stored in sealed vessels for further analysis.

2.1.2 Biofuel burning aerosols

We employed the device depicted in Figure 1 to generate and collect biofuel burning aerosols, and more details can be found elsewhere (Li et al., 2025). It should be noted that biofuel burning experiments this work conducted are designed to simulate domestic biofuel burning, and may not be representative of wildfires (Hamilton et al., 2022). As shown in Figure 1, biofuel was burned in a commercial cook stove, and the smoke generated from biofuel burning passed through a horizontal metal chimney (200 cm in length, 30 cm in inner diameter) and then entered a chamber (50 cm in height, 45 cm in diameter). Air in the chamber was then drawn through a filter bag using a vacuum cleaner to collect aerosol particles. Being different

https://doi.org/10.5194/egusphere-2026-3780
Preprint. Discussion started: 14 July 2026

from our previous work (Li et al., 2025) which used a medium volume aerosol sampler to collect $PM_{2.5}$ samples, the present study employed a vacuum cleaner to collect aerosol particles emitted from biofuel burning (i.e. no size selection was applied), and the purpose was to obtain a sufficient amount of Fe-containing particles for Fe isotopic analysis. Biofuel examined in this work contained no apparent soil particles and was burned in a stove, and the influence of Fe contained in soil particles was minimized.

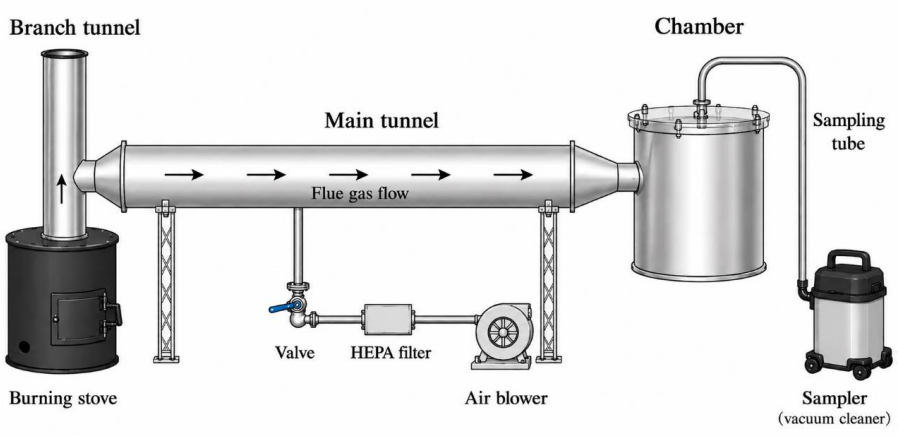

Figure 1. Schematic diagram of the device used in our study to generate and collect biofuel burning aerosols. This figure was created with the assistance of ChatGPT.

Prior to each sample collection, a new filter bag was used for the vacuum cleaner and the sampling tubing was cleaned with ultrapure water, in order to avoid cross-contamination between samples. Each sample was collected over a period of 6-12 h, with final sample mass of 2-5 g. After sampling, filter bags loaded with particles were placed in a desiccator at room temperature for 48 hours to remove moisture, and then stored in sealed vessels for further analysis.

This work examined 11 types of biofuel commonly found in China, consisting of 5 crop straws (wheat, maize, peanut, soybean, and rice) and 6 woods (Chinese fir, birch, pine, lychee,

https://doi.org/10.5194/egusphere-2026-3780
Preprint. Discussion started: 14 July 2026

apple, and pear). One aerosol sample was collected for each biofuel, and thus in total 11 biofuel burning aerosol samples were collected.

2.1.3 Municipal waste fly ash, oil bottom ash, and urban particulate matter

Moreover, this study measured the Fe isotope compositions of another 4 anthropogenic samples. They were a municipal waste fly ash sample (MWFA-FDU) provided by Fudan University (Ding et al., 2019), a certified reference material for waste incineration fly ash (BCR-615) from the Institute for Reference Materials and Measurements (IRMM), a heavy oil bottom ash sample provided by Fudan University (Fu et al., 2012), and a certificated reference material for urban particulate matter (NIST 1648a) from the National Institute of Standards and Technology (NIST).

2.2 Sample pretreatment and chemical purification

Sample pretreatment (mainly digestion) and chemical purification were conducted in a Class 100 ultra-clean laboratory at Guangzhou Institute of Geochemistry, Chinese Academy of Sciences. A brief overview is given below, and further details are provided in the Supplement (Sect. S1).

2.2.1 Sample digestion

Due to low Fe content and high organic matter content, biofuel burning aerosol samples were first heated in a muffle furnace at 900 °C for at least 90 min to remove organic matters they contained; after being cooled down to room temperature, for each sample, 0.5 g of the sample was weighed and then used for subsequent analysis. All the other samples were heated in a muffle furnace at 600°C for at least 60 min; after being cooled down, for each sample, 10-35 mg was weighed and then used for further analysis.

As detailed in the Supplement (Sect. S1.2), except for steelwork fly ash and biofuel burning aerosol, samples examined in this work were digested by a sequential protocol at 120 ^{o}C, using 1) HNO_3-HF, 2) H_2O_2-HNO_3, 3) Aqua Regia, and 4) HCl, respectively. Steelwork

https://doi.org/10.5194/egusphere-2026-3780
Preprint. Discussion started: 14 July 2026

fly ash and biofuel burning aerosol samples contained substantial amounts of carbonaceous or refractory materials, requiring additional pre-digestion to remove carbonaceous materials and microwave-assisted digestion to dissolve refractory materials; as a result, these samples were digested using the following sequential digestion protocol, namely 1) pre-digestion in HNO_3-H_2O_2 at room temperature, 2) microwave-assisted digestion in HNO_3-HF, 3) heated dissolution in Aqua Regia, and 4) heated dissolution in HCl. After digestion, the digestates were diluted with 2.5 mol/L HCl and then subjected to centrifugation, and the resulting solutions were used for the subsequent chemical purification.

2.2.2 Chemical purification

Chemical purification, which minimizes matrix effects and enhances the accuracy of Fe isotope analysis, is an essential step for high-precision Fe isotope analysis. In this study, chemical purification of Fe was achieved using a single column filled with AGMP-50 cation exchange resin (Bio-Rad, USA), as detailed in the Supplement (Sect. S1.3). In brief, the resin column was sequentially cleaned with 6 mol/L HNO_3 (10 mL), 6 mol/L HCl (15 mL), and ultrapure water (5 mL), respectively. It was then conditioned with 0.2 mol/L HCl (1 mL), and after that 100 μL sample solution was loaded into the resin column. Subsequently, HCl-HF (both at 0.2 mol/L, 3 mL) and HCl-HF solution (which contained 0.2 and 0.5 mol/L HCl and HF, 1 mL) were sequentially added into the resin column to elute matrix elements. Finally, 7 mL HCl-HF solution (which contained 0.2 and 0.5 mol/L HCl and HF) was added into the resin column to elute Fe, and the Fe-containing fraction was collected into a clean PFA beaker.

The Fe-containing fraction was then evaporated to dryness, dissolved with 200 μL concentrated HNO_3, and evaporated again to dryness at 120 °C. The obtained residue was then dissolved in 2% HNO_3 for Fe isotope measurement. For the purification procedure employed in this study, the Fe recovery was >98% and the procedural blank was <6 ng (Zhu et al., 2020). This procedural blank was negligible when compared to the amount of Fe our samples

https://doi.org/10.5194/egusphere-2026-3780
Preprint. Discussion started: 14 July 2026

contained (>300 ng).

2.3 Multi-Collector Inductively Coupled Plasma Mass Spectrometry

A multi-collector inductively coupled plasma mass spectrometer (Neptune Plus MC-ICP-MS, Thermo Fisher Scientific) was employed to measure the Fe isotopic compositions of our samples. The sample and standard solutions were diluted to the same Fe concentration (2 μg/g) using 2% HNO_3 (v/v), in order to minimize the measurement errors arising from differences in solution matrix and Fe concentration (Malinovsky et al., 2003; Dauphas et al., 2009). Since argon (Ar) was used as the carrier gas and the solutions to be analyzed contained HNO_3, polyatomic ions (such as $^{40}Ar^{14}N^+$, $^{40}Ar^{16}O^+$, $^{40}Ar^{16}OH^+$, and $^{40}Ar^{18}O^+$) could be generated in high-temperature plasma and would cause isobaric interferences on ^{54}Fe, ^{56}Fe, ^{57}Fe, and ^{58}Fe (Weyer and Schwieters, 2003). To effectively eliminate these isobaric interferences, Fe isotopic measurements were conducted in the pseudo-high-resolution mode (resolution > 14,000) (Zhu et al., 2020).

The standard-sample bracketing (SSB) method was employed to correct for instrumental mass discrimination during the analysis. In addition, the impact of ^{54}Cr on ^{54}Fe was corrected by monitoring the ^{53}Cr signals and using the natural $^{53}Cr/^{54}Cr$ ratio (Weyer and Schwieters, 2003). Fe isotopic compositions are typically reported in δ values, given by Eq. (1):

$$\delta^x Fe(‰)=\left[\frac{(^xFe/^{54}Fe)_{sample}}{(^xFe/^{54}Fe)_{standard}} - 1\right]\times 1000 \qquad (1)$$

where x is 56, 57, or 58. To be consistent with the majority of previous studies (Fitzsimmons and Conway, 2023), Fe isotopic compositions are reported here as $\delta^{56}Fe$ (and $\delta^{57}Fe$) values relative to IRMM-014, thereby facilitating comparison among different studies.

3 Results and discussion

3.1 Measurement precision and accuracy

Figure 1 plots all the $\delta^{56}Fe$ values measured in our work versus $\delta^{57}Fe$, suggesting that $\delta^{57}Fe$ are very well correlated with $\delta^{56}Fe$ which ranged from -1.23‰ to +0.58‰. In addition,

https://doi.org/10.5194/egusphere-2026-3780
Preprint. Discussion started: 14 July 2026

the slope was found to be 1.476±0.014 (1 σ), being very close to the expected value (1.475) (Beard et al., 2003b; Kubik et al., 2021; Zhang et al., 2025).

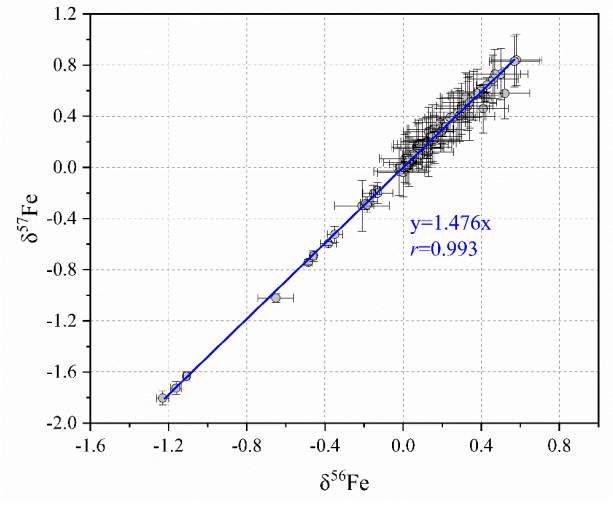

Figure 2. Comparison of $\delta^{56}Fe$ versus $\delta^{57}Fe$ values measured in our work. All the individual measurements (84 in total, including measurements of standards) conducted in this work are presented in this figure.

As shown in Table S2, for the nine standards/samples for which replicate measurements were conducted, the range of $\delta^{56}Fe$ values determined by replicate measurements, defined as the difference between the maximum and minimum values, did not exceed 0.08‰. Such variations were not larger than the uncertainties associated with individual measurements, demonstrating the reproducibility and precision of our $\delta^{56}Fe$ measurements. Moreover, Table 1 shows that our measured $\delta^{56}Fe$ values agreed very well with those reported in literature for the four standards this work our study examined (BRC-2, BHVO-2, SARM4 and GIG-Fe), supporting the accuracy of our $\delta^{56}Fe$ measurements.

Table 1. Comparison of $\delta^{56}Fe$ values measured in our work for standards with those reported

https://doi.org/10.5194/egusphere-2026-3780
Preprint. Discussion started: 14 July 2026

in previous studies. In this table, *n* denotes the number of replicate measurements we performed.

Sample	δ^{56}Fe (‰)	Note
BHVO-2	+0.12±0.13 (n=1)	This work
	+0.13±0.05	(Du et al., 2017)
	+0.11±0.03	(Zhao et al., 2017)
	+0.13±0.03	(Zhu et al., 2020)
BCR-2	+0.10±0.08 (n=2)	This work
	+0.11±0.08	(Du et al., 2017)
	+0.11±0.03	(Liu et al., 2014)
	+0.13±0.02	(Zhu et al., 2020)
SARM4	+0.07±0.08 (n=2)	This work
	+0.09±0.03	(Zhu et al., 2020)
GIG-Fe	+0.71±0.12 (n=1)	This work
	+0.71±0.02	(Zhu et al., 2020)

3.2 Isotopic composition of natural desert dust Fe

In this study, δ^{56}Fe was measured to be +0.01±0.13‰ (n=1) for Saharan dust. As shown in Table 2, the average δ^{56}Fe were measured to be +0.09±0.13‰ and +0.08±0.10‰ for fine (<2.5 μm) and coarse (>2.5 μm) Saharan dust aerosol (n=14) (Mead et al., 2013), and Conway et al. (2019) reported an average δ^{56}Fe of +0.12±0.03‰ (n=13) for Saharan dust aerosol. The Fe isotope composition of Saharan dust measured in our work agree well with these reported in previous work (Mead et al., 2013; Conway et al., 2019). The average δ^{56}Fe was determined to be +0.04±0.07‰ (n=3) for ATD in this study (Table 2), and it was measured previously to be +0.13±0.04‰ (Mead et al., 2013), -0.04±0.10‰ (Li et al., 2022) and +0.06±0.04‰ (Kurisu et al., 2026). The δ^{56}Fe value measured in our work is consistent with those reported in previous studies (Mead et al., 2013; Li et al., 2022; Kurisu et al., 2026), when the overall analytical uncertainties (about ±0.05‰) are taken into account.

Table 2. Comparison of δ^{56}Fe values measured in our work for desert dust with those reported in previous studies. In this table, *n* denotes the number of replicate measurements we performed.

https://doi.org/10.5194/egusphere-2026-3780
Preprint. Discussion started: 14 July 2026

Sample	δ^{56}Fe (‰)	Note
Saharan dust	+0.01±0.13 (n=1)	This work
	+0.09±0.13 (<2.5 μm)	(Mead et al., 2013)
	+0.08±0.10 (>2.5 μm)	(Mead et al., 2013)
	+0.12±0.03	(Conway et al., 2019)
Arizona test dust	+0.04±0.07 (n=3)	This work
	+0.13±0.04	(Mead et al., 2013)
	-0.04±0.10	(Li et al., 2022)
	+0.06±0.04	(Kurisu et al., 2026)
Luochuan loess	+0.14±0.03 (n=2)	This work
Loess	+0.13±0.06	(Beard et al., 2003a)
Loess and paleosol	+0.09±0.03	(Gong et al., 2017)
Taklamakan dust	+0.14±0.13 (n=1)	This work
Gobi dust	+0.30±0.13 (n=1)	This work
Qinghai dust	+0.19±0.13 (n=1)	This work
Tibet dust	+0.16±0.13 (n=1)	This work
TLF dust	+0.21±0.05 (n=1)	(Li et al., 2022)

Our work found the Luochuan loess in China to have an average δ^{56}Fe of +0.14 ± 0.03‰ (n=2). The average δ^{56}Fe was determined to be +0.13±0.06‰ for loess samples (n=10) from different regions of the world (Beard et al., 2003a) and +0.09±0.03‰ for loess and paleosol samples (n=32) from the Chinese Loess Plateau (Gong et al., 2017). Our measured δ^{56}Fe of loess agrees well with previous studies (Beard et al., 2003a; Gong et al., 2017). Among the four Chinese dust samples we examined (Table 2), δ^{56}Fe were measured to be +0.14±0.13‰, +0.19±0.13‰, and +0.16±0.13‰ for Taklamakan dust, Qinghai dust, and Tibet dust, in good agreement with that for TLF dust (+0.21±0.05‰) reported in our previous work (Li et al., 2022). Gobi dust was found in our work to have a δ^{56}Fe value of +0.30±0.13‰, which is broadly comparable with those for other dust samples.

https://doi.org/10.5194/egusphere-2026-3780
Preprint. Discussion started: 14 July 2026

In summary, the average and median δ^{56}Fe were found to be +0.14±0.10‰ (1σ) and +0.14‰ for the seven dust samples we studied (Table 3), and δ^{56}Fe values fell into a small range (+0‰ to +0.2‰) for most samples. Our experimental measurements support the view that the average Fe isotopic composition of desert dust is close to that of UCC (+0.09 ± 0.10‰) (Beard et al., 2003b; Beard and Johnson, 2004; Poitrasson, 2006).

Table 3. Summary of our measured δ^{56}Fe values (in ‰) for natural desert dust, power plant coal fly ash, steelwork fly ash, biofuel burning aerosol, municipal waste fly ash, heavy oil bottom ash, and urban particulate matter. In this table, *n* denotes the number of samples we investigated for each sample type; for steelwork fly ash, this table does not include the 3 samples from the coking process (see Section 3.3.2 for more details).

sample type	*n*	range	average	median
natural desert dust	7	+0.01 to +0.30	+0.14±0.10	+0.14
power plant coal fly ash	28	-0.20 to +0.57	+0.26±0.18	+0.28
steelwork fly ash	18	-1.16 to +0.29	-0.07±0.41	+0.04
biofuel burning aerosol	11	-1.23 to +0.21	-0.28±0.39	-0.15
municipal waste fly ash	2	+0.08 to +0.32	+0.20±0.12	+0.20
heavy oil bottom ash	1	+0.38	/	/
urban particulate matter	1	+0.08	/	/

3.3 Isotopic composition of anthropogenic and combustion Fe

3.3.1 Power plant coal fly ash

For the 28 power plant coal fly ash samples we investigated, δ^{56}Fe ranged from -0.20‰ to +0.57‰ (Table S3), showing considerable variation, and the median and average values were found to be +0.28‰ and +0.26±0.18‰ (1σ) (Table 3). The three coal fly ash samples Mead et al. (2013) investigated had δ^{56}Fe values of +0.22±0.10‰, +0.22±0.06‰, and +0.61±0.08‰, with the average being +0.35±0.23‰. Li et al. (2022) found δ^{56}Fe to be

https://doi.org/10.5194/egusphere-2026-3780
Preprint. Discussion started: 14 July 2026

+0.05±0.08‰, +0.20±0.07‰, and +0.75±0.01‰ for one Chinese and two American coal fly ash samples, with an average value of +0.33±0.37‰. Our measured δ^{56}Fe values have large overlaps with these reported by the two previous studies (Mead et al., 2013; Li et al., 2022), although the average δ^{56}Fe we reported is slightly lower.

As shown in Table 3, our work suggests that the δ^{56}Fe values have substantial overlaps for power plant coal fly ash (-0.20‰ to +0.57‰) and desert dust (+0.01‰ to +0.30‰), while the average δ^{56}Fe is higher for coal fly ash (+0.26±0.18‰) than desert dust (+0.14±0.10‰). This implies that coal fly ash Fe could be isotopically heavier (at least not lighter) than desert dust Fe.

3.3.2 Steelwork fly ash

The 21 steelwork fly ash samples we studied showed large variation in δ^{56}Fe (-1.16‰ to +0.43‰) (Table S4), with average and median values being +0.00±0.42‰ (1σ) and +0.09‰. Among the 21 samples, δ^{56}Fe were measured to be +0.39‰, +0.42‰, and +0.43‰ for the three coking fly ash samples, with an average of +0.42±0.04‰ (1σ), being much higher than the other 18 steelwork fly ash samples. This difference can be attributed to the fact that coking process (during which coal is pyrolyzed in an oxygen-free environment to produce coke) uses coal as the main raw material (Keboletse et al., 2021), and thus Fe composition of the generated fly ash is different from that produced in other steelwork processes. In fact, the average δ^{56}Fe (+0.42±0.04‰, 1σ) we determined for coking fly ash is rather close to that for power plant coal fly ash (+0.26±0.18‰, 1σ), implying that they originated from the same raw material (i.e. coal).

For the other 18 steelwork fly ash samples we examined, δ^{56}Fe ranged from -1.16‰ to +0.29‰, and the median and average values were determined to be +0.04‰ and -0.07±0.41‰ (1σ) (Table 3). The average δ^{56}Fe value was reported to be +0.08±0.24‰ (n=10) (Flament et al., 2008) and -0.12±0.08‰ (n=4) for steelwork fly ash (Maters et al., 2022), aligning fairly well with our result. Compared to desert dust, although a few samples were enriched in

https://doi.org/10.5194/egusphere-2026-3780
Preprint. Discussion started: 14 July 2026

isotopically heavier Fe, most steelwork fly ash in general shows slightly lower or similar δ^{56}Fe values; therefore, aerosol Fe emitted by steelworks may be a potential source of isotopically light Fe observed in the tropospheric aerosols.

3.3.3 Biofuel burning aerosol

This study determined the Fe isotopic composition of 11 biofuel burning aerosol samples (Table S5). As mentioned in Section 2.1.2, biofuel burning experiments conducted in this work are designed to simulate domestic biofuel burning, and may not be representative of wildfires, which can also entrain soil particles into the atmosphere (Hamilton et al., 2022; Bunnell et al., 2025). The lowest and highest δ^{56}Fe values (-1.23‰ versus +0.21‰) were found for pear wood and soybean straw burning aerosol, respectively. As shown in Table 3, the median and average δ^{56}Fe were determined to be -0.15‰ and -0.28±0.39‰ (1σ), lower than that of desert dust (+0.14±0.10‰). Most biofuel burning aerosol samples we examined exhibited δ^{56}Fe below 0‰, showing significant enrichment of isotopically lighter Fe. In contrast, a previous study (Kurisu and Takahashi, 2019) found average δ^{56}Fe to be +0.09±0.03‰ for reed residual ash (and +0.08±0.10‰ for reed), being very similar to the UCC and thus indicating no obvious enrichment of lighter Fe.

Plants use Strategy I or II to absorb Fe from soil (Kobayashi and Nishizawa, 2012). It was suggested that compared to the soil where plants are grown, Strategy I plants are usually enriched in isotopically lighter Fe while Strategy II plants are relatively enriched in the heavier Fe (Guelke and Von Blanckenburg, 2007). Eight Strategy I plants, namely peanut, soybean, birch, lychee wood, apple wood, pear wood, fir, and pine, were examined in our work, and the average δ^{56}Fe was determined to be -0.22±0.47‰ (1σ, n=8) for the corresponding biofuel burning aerosols. We also investigated three Strategy II plants, namely wheat, corn, and rice straw, and the average δ^{56}Fe was determined to be -0.33±0.28‰ (1σ, n=3) for the corresponding biofuel burning aerosol. Based on the data our work obtained, our work suggests

https://doi.org/10.5194/egusphere-2026-3780
Preprint. Discussion started: 14 July 2026

that δ^{56}Fe values of biofuel burning aerosols generated from Strategy I plants are not significantly different from those for Strategy II plants ($p>0.05$). Our result seems to deviate from what was reported by Guelke and Von Blanckenburg (2007), probably because biofuel we studied were grown from different soils which may have different Fe isotopic compositions (Johnson et al., 2020). In addition, the number of biofuel burning samples analyzed in our study is relatively limited, and further measurements are required to confirm our finding.

3.3.4 Other samples

For the two municipal incineration fly ash samples we examined, δ^{56}Fe were measured to be +0.32±0.06‰ and +0.08±0.13‰ (Table 3), respectively, with an average value of +0.20±0.12‰ (1σ). Kurisu et al. (2016b) found δ^{56}Fe to be -0.08±0.09‰ and -0.10±0.03‰ for municipal incineration bottom and fly ash from Japan, slightly lower than our result. Li et al. (2022) found δ^{56}Fe to be +0.10±0.08‰ for a European municipal incineration fly ash sample (BCR-176R), close to that obtained in our current study. Overall, available studies suggest relatively large variations in δ^{56}Fe for municipal incineration fly ash, ranging from -0.10‰ to +0.32‰.

The δ^{56}Fe value was measured to be +0.38±0.13‰ for the heavy oil bottom ash sample we examined (Table 3), similar to that for oil fly ash (+0.30±0.17‰, n=4) reported by Mead et al. (2013). NIST 1648a and NIST 1649a are both certificated urban particulate matter provided by NIST. The δ^{56}Fe was measured by our work to be +0.08±0.13‰ for NIST 1648a (Table 3), in good agreement with those reported for NIST 1649a (+0.00±0.03‰ and +0.01±0.12‰, respectively) by two previous studies (Beard et al., 2003a; Mead et al., 2013).

3.4 Discussion

3.4.1 Atmospheric implications

Figure 3 summarizes the Fe isotopic composition of natural desert dust and several important anthropogenic particles our work investigated. Mead et al. (2013) proposed biomass

https://doi.org/10.5194/egusphere-2026-3780
Preprint. Discussion started: 14 July 2026

burning as the most likely source of isotopically light Fe observed in the troposphere, since plant matter is the sole material known to contain light Fe. Nevertheless, at that time no measurement of δ^{56}Fe endmember values was available. Here we found that δ^{56}Fe values ranged from -1.23‰ to +0.21‰ (average: -0.28±0.39‰, 1σ) for the 11 biofuel burning aerosol samples examined in this work, lower than natural desert dust. Thus, our work suggests that biofuel burning aerosol could be an potentially important source of light Fe in the troposphere, providing experimental results to support what Mead et al. (2013) proposed. The lowest δ^{56}Fe we reported for domestic biofuel burning was -1.23‰, while δ^{56}Fe could be lower than -3‰ for soluble Fe in tropospheric aerosols (Kurisu et al., 2016a; Hsieh and Ho, 2024). This indicates that biofuel burning alone cannot explain the very light Fe observed for tropospheric aerosols, i.e. other sources/processes are needed.

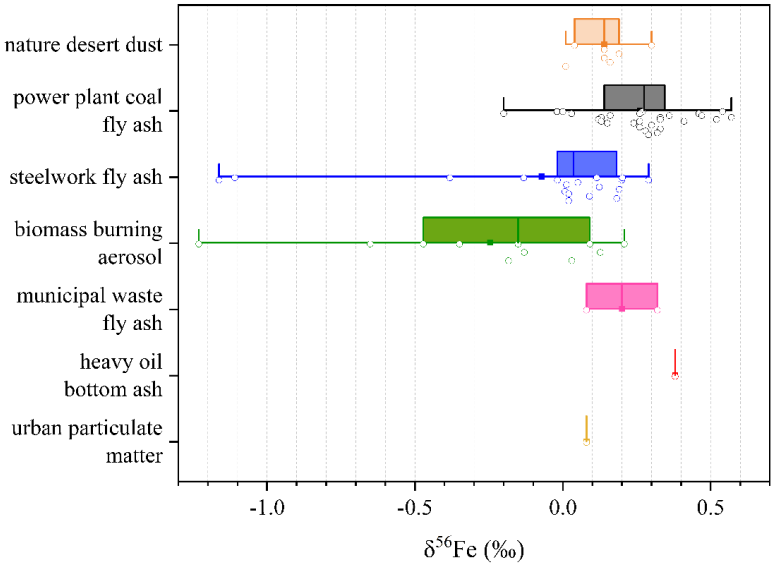

Figure 3. Summary of δ^{56}Fe values measured in our work for natural desert dust (n=7), power plant coal fly ash (n=28), steelwork fly ash (n=18, and the three samples from the coking process were not included), biofuel burning aerosol (n=11), municipal waste fly ash (n=2),

https://doi.org/10.5194/egusphere-2026-3780
Preprint. Discussion started: 14 July 2026

heavy oil bottom ash (n=1), and urban particulate matter (n=1).

In addition to domestic biofuel burning, there are other types of biomass burning, such as wildfire and open burning of agricultural straws. Our study represents domestic biofuel burning well. On the other hand, soil and biomass Fe both contribute substantially to aerosol Fe emitted by wildfires (Kurisu and Takahashi, 2019; Hamilton et al., 2022), and therefore wildfire aerosol Fe may have δ^{56}Fe endmember values different from that we report for domestic biofuel burning aerosol.

The 28 power plant coal fly ash samples we examined had δ^{56}Fe in the range of -0.20‰ to +0.57‰ (average: +0.26±0.18‰, 1σ), indicating that power plant coal fly ash is usually enriched in heavier Fe. As a result, we suggest that not all the anthropogenic aerosol Fe is isotopically lighter than desert dust Fe, in contrast to what previous studies usually assumed. Tropospheric aerosol Fe typically exhibits similar or lower δ^{56}Fe values relative to desert dust; nevertheless, higher values have been reported in a few studies (Labatut et al., 2014; Bunnell et al., 2025; Camin et al., 2025), the causes of which are still under debate. Based on δ^{56}Fe endmember values our work reported, we suggest that coal-fired power plant emission can potentially (at least partly) explain the higher δ^{56}Fe values observed for aerosol Fe in the troposphere.

The average δ^{56}Fe was -0.07±0.41‰ (1σ) for the 18 steelwork fly ash samples we examined (excluding the three samples collected from the coking process). Compared to desert dust, most steelwork fly ash samples had slightly lower or similar δ^{56}Fe (ranging from -1.16‰ to +0.29‰) (Figure 3), and thus may contribute to lighter Fe observed for tropospheric aerosols.

Compared to desert dust, municipal incineration fly ash, heavy oil combustion bottom ash, and urban particulate matter our work examined had similar or higher δ^{56}Fe (Figure 3), but the small sample sizes preclude us from drawing further conclusions.

https://doi.org/10.5194/egusphere-2026-3780
Preprint. Discussion started: 14 July 2026

3.4.2 Recommendations for future work

Biofuel burning aerosol samples this work used were aerosol particles emitted by biofuel burning in a commercial stove, thereby being of direct atmospheric relevance. Instead of aerosol particles, fly ash samples were used to represent particulate matters emitted by coal-fired power plants and steelwork. Their volume mean diameters were mostly a few tens of μm (Li et al., 2025), considerably larger than these for tropospheric aerosols (typically a few μm or less). Kurisu et al. (2016b) found δ^{56}Fe to be much lower for TSP than fly ash collected in an incinerator, possibly due to enrichment of lighter Fe in aerosol particles caused by the evaporation-condensation process in combustion. This hypothesis was further supported by a following study (Kurisu et al., 2019), which found that δ^{56}Fe was much lower in the fine mode (<1.3μm) than the coarse mode (>1.3 μm) for aerosol particles collected at a site which was ~4 km from a steel plant. If the hypothesis proposed by Kurisu et al. (2016b) is correct, then the actual δ^{56}Fe endmember values for coal-fired power plant and steelwork emission could be lower than these reported in our work.

It is noted that an earlier study (Flament et al., 2008) did not support what was proposed by Kurisu et al. (2016b). In fact, Flament et al. (2008) observed no significant Fe fractionation during steelwork processes, and found the average δ^{56}Fe of total Fe to be +0.14±0.11‰ (1σ, n=6) for aerosol particles collected at a site which was ~5 km from a major steelwork plant, being similar to (or even slightly larger than) that for desert dust Fe. Further measurements of δ^{56}Fe values of aerosol particles emitted by anthropogenic sources, especially size-resolved aerosol particles, can be very valuable.

4 Conclusion

Aerosol Fe, emitted from natural and anthropogenic sources, has remarkable impacts on atmospheric chemistry, human health and marine biogeochemistry, while quantitative source apportionment of total and soluble aerosol Fe is still a big challenge. In the two decades Fe

https://doi.org/10.5194/egusphere-2026-3780
Preprint. Discussion started: 14 July 2026

444 isotopes have been increasingly utilized for source apportionment of aerosol Fe, showing great
445 advantages. The δ^{56}Fe endmember values for anthropogenic aerosol Fe are critical for using Fe
446 isotopes for apportionment of aerosol Fe, but are poorly constrained for anthropogenic
447 emissions due to the lack of experimental measurements.

448 In this work, we measured and reported isotopic composition of aerosol Fe from several
449 important anthropogenic sources. For the seven desert dust samples we investigated, δ^{56}Fe
450 values ranged from +0.01 to +0.30‰ with an average value of +0.14±0.10‰ (1σ), supporting
451 that Fe isotopic composition of desert dust is rather homogeneous and close to that of crustal
452 materials (+0.09±0.10‰). Compared to desert dust, the average δ^{56}Fe was determined to be
453 +0.26±0.18‰ (1σ) for power plant coal fly ash (n=28). This implies that not all the
454 anthropogenic Fe is isotopically lighter than desert dust Fe, and that coal-fired power plant
455 emission can be one potential reason to explain the higher δ^{56}Fe values observed for aerosol Fe
456 in the troposphere. The average δ^{56}Fe was found in our work to be -0.07±0.41‰ (1σ) for
457 steelwork fly ash (n=18), being slightly lower than desert dust Fe; it was reported to
458 be -0.28±0.39‰ (1σ) for biofuel burning aerosol (n=11), considerably lower for desert dust.
459 As a result, one may conclude that emission from steelwork and biofuel burning both could be
460 important sources for the lighter Fe observed in the troposphere.

461 Based on Fe isotopic data, previous studies usually utilized the two-component mixing
462 model for aerosol Fe source apportionment (Conway et al., 2019; Hsieh and Ho, 2024; Kurisu
463 et al., 2024; Shuai et al., 2025; Kurisu et al., 2026). The two-component mixing model assigned
464 a single δ^{56}Fe endmember value to the anthropogenic source. Our work reveals large
465 differences in the average δ^{56}Fe values among power plant coal fly ash, steelwork fly ash, and
466 biofuel burning aerosol; furthermore, substantial variations in δ^{56}Fe values are also observed
467 among individual samples within each type of these anthropogenic sources. Compared to the
468 simple two-component mixing model, the Bayesian MixSIAR model (Wang et al., 2022; Wei

https://doi.org/10.5194/egusphere-2026-3780
Preprint. Discussion started: 14 July 2026

et al., 2024), which can incorporate δ^{56}Fe endmember values for multiple sources and account for their associated uncertainties, could offer distinct advantages for the quantification of aerosol Fe sources.

Our work also has some caveats. In addition to domestic biofuel burning, there are other types of biomass burning, such as wildfire and open burning of agricultural straws. Since wildfires can entrain both soil and biomass Fe into the atmosphere (Kurisu and Takahashi, 2019; Hamilton et al., 2022), wildfire aerosol Fe may exhibit δ^{56}Fe endmembers which differ from those for domestic biofuel burning. We also note that the lowest δ^{56}Fe endmember value measured in our work was only -1.23‰ (Table 3), implying that other sources/processes are needed to explain the very low δ^{56}Fe values (sometimes lower than -3‰) aerosol Fe in the troposphere. Furthermore, our work only measured δ^{56}Fe endmember values of total aerosol Fe from different sources. Previous studies have generally assumed that for any given source, the δ^{56}Fe endmember values are identical for total and soluble Fe. This assumption, however, is not necessarily valid since isotopic fractionation may occur during dissolution; therefore, simultaneous measurements of isotopic composition of total and soluble Fe are warranted for various sources. Finally, as discussed in Section 3.4.2, compared to aerosol particles in the troposphere, power plant coal fly ash and steelwork fly ash samples we examined have considerably larger diameters, and thus our result may not be fully representative. Experimental measurements of δ^{56}Fe values for aerosol particles emitted by anthropogenic sources, and size-resolved measurements in particular, would be very valuable in providing reliable constraint on δ^{56}Fe endmember values.

Data availability.

Data used in this work can be found in the manuscript or the supplement.

Author contribution.

https://doi.org/10.5194/egusphere-2026-3780
Preprint. Discussion started: 14 July 2026

MT designed this study; YZ, GZ, RL, TZ, YC, and JM conducted experimental work; ML and YY provided key samples used in this work; XM and MT secured funding resources; YZ, GZ, JM, and MT analyzed the result and wrote the manuscript; all the authors reviewed and approved the manuscript.

Competing interests.

At least one of the (co-)authors is a member of the editorial board of Atmospheric Chemistry and Physics.

Acknowledgements.

We would like to thank Professor Mei Li at Jinan University (Guangzhou, China) for kindly providing some samples examined in this work.

Financial support.

This work was sponsored by National Natural Science Foundation of China (42321003, 42405111 and 42507154), International Partnership Program of Chinese Academy of Sciences (164GJHZ2024011FN), and Guangzhou Bureau of Science and Technology (2024A04J6533).

https://doi.org/10.5194/egusphere-2026-3780
Preprint. Discussion started: 14 July 2026

References

Al-Abadleh, H. A.: Iron content in aerosol particles and its impact on atmospheric chemistry, Chem. Commun., 60, 1840-1855, 10.1039/d3cc04614a, 2024.

Beard, B. L. and Johnson, C. M.: Fe isotope variations in the modern and ancient earth and other planetary bodies, in: Geochemistry of Non-Traditional Stable Isotopes, edited by: Johnson, C. M., Beard, B. L., and Albarede, F., Reviews in Mineralogy & Geochemistry, 319-357, 10.2138/gsrmg.55.1.319, 2004.

Beard, B. L., Johnson, C. M., Von Damm, K. L., and Poulson, R. L.: Iron isotope constraints on Fe cycling and mass balance in oxygenated Earth oceans, Geology, 31, 629-632, 10.1130/0091-7613(2003)031<0629:Iicofc>2.0.Co;2, 2003a.

Beard, B. L., Johnson, C. M., Skulan, J. L., Nealson, K. H., Cox, L., and Sun, H.: Application of Fe isotopes to tracing the geochemical and biological cycling of Fe, Chem. Geol., 195, 87-117, 10.1016/s0009-2541(02)00390-x, 2003b.

Boyd, P. W. and Ellwood, M. J.: The biogeochemical cycle of iron in the ocean, Nat. Geosci., 3, 675-682, 10.1038/ngeo964, 2010.

Boyd, P. W., Jickells, T., Law, C. S., Blain, S., Boyle, E. A., Buesseler, K. O., Coale, K. H., Cullen, J. J., de Baar, H. J. W., Follows, M., Harvey, M., Lancelot, C., Levasseur, M., Owens, N. P. J., Pollard, R., Rivkin, R. B., Sarmiento, J., Schoemann, V., Smetacek, V., Takeda, S., Tsuda, A., Turner, S., and Watson, A. J.: Mesoscale iron enrichment experiments 1993-2005: Synthesis and future directions, Science, 315, 612-617, 10.1126/science.1131669, 2007.

Bunnell, Z. B., Sieber, M., Hamilton, D. S., Marsay, C. M., Buck, C. S., Landing, W. M., John, S. G., and Conway, T. M.: The Influence of Natural, Anthropogenic, and Wildfire Sources on Iron and Zinc Aerosols Delivered to the North Pacific Ocean, Geophys. Res. Lett., 52, e2024GL113877, 10.1029/2024GL113877, 2025.

Camin, C., Lacan, F., Pradoux, C., Labatut, M., Johansen, A., and Murray, J. W.: Iron isotopes suggest significant aerosol dissolution over the Pacific Ocean, Atmos. Chem. Phys., 25, 8213-8228, 10.5194/acp-25-8213-2025, 2025.

Chen, L. X. D., Peng, C., Gu, W. J., Fu, H. J., Jian, X., Zhang, H. H., Zhang, G. H., Zhu, J. X., Wang, X. M., and Tang, M. J.: On mineral dust aerosol hygroscopicity, Atmos. Chem. Phys., 20, 13611-13626, 10.5194/acp-20-13611-2020, 2020.

Chen, Y., Wang, Z., Fang, Z., Huang, C., Xu, H., Zhang, H., Zhang, T., Wang, F., Luo, L., Shi, G., Wang, X., and Tang, M.: Dominant Contribution of Non-dust Primary Emissions and Secondary Processes to Dissolved Aerosol Iron, Environ. Sci. Technol., 58, 17355-17363, 10.1021/acs.est.4c05816, 2024.

Conway, T. M., Hamilton, D. S., Shelley, R. U., Aguilar-Islas, A. M., Landing, W. M., Mahowald, N. M., and John, S. G.: Tracing and constraining anthropogenic aerosol iron fluxes to the North Atlantic Ocean using iron isotopes, Nat. Commun., 10, 2628, 10.1038/s41467-019-10457-w, 2019.

Dauphas, N., Pourmand, A., and Teng, F.: Routine isotopic analysis of iron by HR-MC-ICPMS: How precise and how accurate, Chem. Geol., 267, 175-184, 10.1016/j.chemgeo.2008.12.011, 2009.

Ding, X., Li, Q., Wu, D., Liang, Y. G., Xu, X. M., Xie, G. Z., Wei, Y. Q., Sun, H., Zhu, C., Fu, H. B., and

https://doi.org/10.5194/egusphere-2026-3780
Preprint. Discussion started: 14 July 2026

Chen, J. M.: Unexpectedly Increased Particle Emissions from the Steel Industry Determined by Wet/Semidry/Dry Flue Gas Desulfurization Technologies, Environ. Sci. Technol., 53, 10361-10370, 10.1021/acs.est.9b03081, 2019.

Du, D., Wang, X., Yang, T., Chen, X., Li, J., and Li, W.: Origin of heavy Fe isotope compositions in high-silica igneous rocks: A rhyolite perspective, Geochim. Cosmochim. Acta, 218, 58-72, 10.1016/j.gca.2017.09.014, 2017.

Fitzsimmons, J. N. and Conway, T. M.: Novel Insights into Marine Iron Biogeochemistry from Iron Isotopes, Annu. Rev. Mar. Sci., 15, 383-406, 10.1146/annurev-marine-032822-103431, 2023.

Flament, P., Mattielli, N., Aimoz, L., Choel, M., Deboudt, K., de Jong, J., Rimetz-Planchon, J., and Weis, D.: Iron isotopic fractionation in industrial emissions and urban aerosols, Chemosphere, 73, 1793-1798, 10.1016/j.chemosphere.2008.08.042, 2008.

Fu, H., Lin, J., Shang, G., Dong, W., Grassian, V. H., Carmichael, G. R., Li, Y., and Chen, J.: Solubility of Iron from Combustion Source Particles in Acidic Media Linked to Iron Speciation, Environ. Sci. Technol., 46, 11119-11127, 10.1021/es302558m, 2012.

Gong, Y., Xia, Y., Huang, F., and Yu, H.: Average iron isotopic compositions of the upper continental crust: constrained by loess from the Chinese Loess Plateau, Acta Geochim., 36, 125-131, 2017.

Guelke, M. and Von Blanckenburg, F.: Fractionation of stable iron isotopes in higher plants, Environ. Sci. Technol., 41, 1896-1901, 10.1021/es062288j, 2007.

Hamilton, D. S., Perron, M. M. G., Bond, T. C., Bowie, A. R., Buchholz, R. R., Guieu, C., Ito, A., Maenhaut, W., Myriokefalitakis, S., Olgun, N., Rathod, S. D., Schepanski, K., Tagliabue, A., Wagner, R., and Mahowald, N. M.: Earth, Wind, Fire, and Pollution: Aerosol Nutrient Sources and Impacts on Ocean Biogeochemistry, Annu. Rev. Mar. Sci., 14, 303-330, 10.1146/annurev-marine-031921-013612, 2022.

Hsieh, C. C. and Ho, T. Y.: Contribution of Anthropogenic and Lithogenic Aerosol Fe in the East China Sea, J. Geophys. Res. Oceans, 129, e2024JC021113, 10.1029/2024jc021113, 2024.

Ito, A., Myriokefalitakis, S., Kanakidou, M., Mahowald, N. M., Scanza, R. A., Hamilton, D. S., Baker, A. R., Jickells, T., Sarin, M., Bikkina, S., Gao, Y., Shelley, R. U., Buck, C. S., Landing, W. M., Bowie, A. R., Perron, M. M. G., Guieu, C., Meskhidze, N., Johnson, M. S., Feng, Y., Kok, J. F., Nenes, A., and Duce, R. A.: Pyrogenic iron: The missing link to high iron solubility in aerosols, Sci. Adv., 5, eaau7671, 10.1126/sciadv.aau7671, 2019.

Jickells, T. D., An, Z. S., Andersen, K. K., Baker, A. R., Bergametti, G., Brooks, N., Cao, J. J., Boyd, P. W., Duce, R. A., Hunter, K. A., Kawahata, H., Kubilay, N., laRoche, J., Liss, P. S., Mahowald, N., Prospero, J. M., Ridgwell, A. J., Tegen, I., and Torres, R.: Global iron connections between desert dust, ocean biogeochemistry, and climate, Science, 308, 67-71, 10.1126/science.1105959, 2005.

Johnson, C., Beard, B., and Weyer, S.: Iron geochemistry: an isotopic perspective, Springer2020.

Keboletse, K. P., Ntuli, F., and Oladijo, O. P.: Influence of coal properties on coal conversion processes-coal carbonization, carbon fiber production, gasification and liquefaction technologies: a review, Int. J. Coal Sci. Technol., 8, 817-843, 10.1007/s40789-020-00401-5, 2021.

Kobayashi, T. and Nishizawa, N. K.: Iron Uptake, Translocation, and Regulation in Higher Plants, in: Annual

https://doi.org/10.5194/egusphere-2026-3780
Preprint. Discussion started: 14 July 2026

Review of Plant Biology, Vol 63, edited by: Merchant, S. S., Annual Review of Plant Biology, 131-152, 10.1146/annurev-arplant-042811-105522, 2012.

Kubik, E., Moynier, F., Paquet, M., and Siebert, J.: Iron Isotopic Composition of Biological Standards Relevant to Medical and Biological Applications, Front. Med., 8, 696367, 10.3389/fmed.2021.696367, 2021.

Kurisu, M. and Takahashi, Y.: Testing Iron Stable Isotope Ratios as a Signature of Biomass Burning, Atmosphere, 10, 76, 10.3390/atmos10020076, 2019.

Kurisu, M., Adachi, K., Sakata, K., and Takahashi, Y.: Stable Isotope Ratios of Combustion Iron Produced by Evaporation in a Steel Plant, Acs Earth and Space Chemistry, 3, 588-598, 10.1021/acsearthspacechem.8b00171, 2019.

Kurisu, M., Takahashi, Y., Iizuka, T., and Uematsu, M.: Very low isotope ratio of iron in fine aerosols related to its contribution to the surface ocean, J. Geophys. Res. Atmos., 121, 11119-11136, 10.1002/2016jd024957, 2016a.

Kurisu, M., Sakata, K., Uematsu, M., Ito, A., and Takahashi, Y.: Contribution of combustion Fe in marine aerosols over the northwestern Pacific estimated by Fe stable isotope ratios, Atmos. Chem. Phys., 21, 16027-16050, 10.5194/acp-21-16027-2021, 2021.

Kurisu, M., Sakata, K., Miyamoto, C., Takaku, Y., Iizuka, T., and Takahashi, Y.: Variation of Iron Isotope Ratios in Anthropogenic Materials Emitted through Combustion Processes, Chem. Lett., 45, 970-972, 10.1246/cl.160451, 2016b.

Kurisu, M., Sakata, K., Nishioka, J., Obata, H., Conway, T. M., Hunt, H. R., Sieber, M., Suzuki, K., Kashiwabara, T., Kubo, S., Takada, M., and Takahashi, Y.: Source and fate of atmospheric iron supplied to the subarctic North Pacific traced by stable iron isotope ratios, Geochim. Cosmochim. Acta, 378, 168-185, 10.1016/j.gca.2024.06.009, 2024.

Kurisu, M., Zhu, C., Miyakawa, T., Ito, A., Suzuki, K., Kashiwabara, T., Kubo, S., Takahashi, Y., Harada, N., Foret, G., Dubois, N., and Kanaya, Y.: Identification of anthropogenic Fe originated from East Asia using Fe stable isotope ratios of aerosols collected on Fukue Island, Atmos. Environ., 373, 121893, 10.1016/j.atmosenv.2026.121893, 2026.

Labatut, M., Lacan, F., Pradoux, C., Chmeleff, J., Radic, A., Murray, J. W., Poitrasson, F., Johansen, A. M., and Thil, F.: Iron sources and dissolved-particulate interactions in the seawater of the Western Equatorial Pacific, iron isotope perspectives, Glob. Biogeochem. Cycles, 28, 1044-1065, 10.1002/2014gb004928, 2014.

Li, R., Zhang, H., Wang, F., He, Y., Huang, C., Luo, L., Dong, S., Jia, X., and Tang, M.: Mass fractions, solubility, speciation and isotopic compositions of iron in coal and municipal waste fly ash, Sci. Total Environ., 838, 155974, 10.1016/j.scitotenv.2022.155974, 2022.

Li, R., Plaas, H. E., Zhang, Y., Chen, Y., Zhang, T., Yang, Y., Rathod, S., Zhang, G., Wang, X., Hamilton, D. S., and Tang, M.: Residential burning is a significant source of soluble iron to the ocean, EGUsphere, 2025, 1-52, 10.5194/egusphere-2025-4058, 2025.

Liu, S. A., Teng, F. Z., Li, S. G., Wei, G. J., Ma, J. L., and Li, D. D.: Copper and iron isotope fractionation

https://doi.org/10.5194/egusphere-2026-3780
Preprint. Discussion started: 14 July 2026

during weathering and pedogenesis: Insights from saprolite profiles, Geochim. Cosmochim. Acta, 146, 59-75, 10.1016/j.gca.2014.09.040, 2014.

Mahowald, N. M., Hamilton, D. S., Mackey, K. R. M., Moore, J. K., Baker, A. R., Scanza, R. A., and Zhang, Y.: Aerosol trace metal leaching and impacts on marine microorganisms, Nat. Commun., 9, 2614, 10.1038/s41467-018-04970-7, 2018.

Malinovsky, D., Stenberg, A., Rodushkin, I., Andren, H., Ingri, J., Öhlander, B., and Baxter, D. C.: Performance of high resolution MC-ICP-MS for Fe isotope ratio measurements in sedimentary geological materials, J. Anal. At. Spectrom., 18, 687-695, 10.1039/b302312e, 2003.

Maters, E. C., Mulholland, D. S., Flament, P., de Jong, J., Mattielli, N., Deboudt, K., Dhont, G., and Bychkov, E.: Laboratory study of iron isotope fractionation during dissolution of mineral dust and industrial ash in simulated cloud water, Chemosphere, 299, 134472, 10.1016/j.chemosphere.2022.134472, 2022.

Mead, C., Herckes, P., Majestic, B. J., and Anbar, A. D.: Source apportionment of aerosol iron in the marine environment using iron isotope analysis, Geophys. Res. Lett., 40, 5722-5727, 10.1002/2013gl057713, 2013.

Moore, C. M., Mills, M. M., Arrigo, K. R., Berman-Frank, I., Bopp, L., Boyd, P. W., Galbraith, E. D., Geider, R. J., Guieu, C., Jaccard, S. L., Jickells, T. D., La Roche, J., Lenton, T. M., Mahowald, N. M., Maranon, E., Marinov, I., Moore, J. K., Nakatsuka, T., Oschlies, A., Saito, M. A., Thingstad, T. F., Tsuda, A., and Ulloa, O.: Processes and patterns of oceanic nutrient limitation, Nat. Geosci., 6, 701-710, 10.1038/ngeo1765, 2013.

Poitrasson, F.: On the iron isotope homogeneity level of the continental crust, Chem. Geol., 235, 195-200, 10.1016/j.chemgeo.2006.06.010, 2006.

Rathod, S. D., Hamilton, D. S., Mahowald, N. M., Klimont, Z., Corbett, J. J., and Bond, T. C.: A Mineralogy-Based Anthropogenic Combustion-Iron Emission Inventory, J. Geophys. Res. Atmos., 125, e2019JD032114, 10.1029/2019jd032114, 2020.

Shuai, W., Zhang, K., Zhang, T., Zheng, W., Liu, Y., Lang, Y., Fu, P., Feng, Y., Peng, J., and Chen, J.: Unraveling the Origin of Atmospheric Soluble Iron during Asian Dust Storms, Environ. Sci. Technol., 59, 23962-23973, 10.1021/acs.est.5c10539, 2025.

Tagliabue, A., Bowie, A. R., Boyd, P. W., Buck, K. N., Johnson, K. S., and Saito, M. A.: The integral role of iron in ocean biogeochemistry, Nature, 543, 51-59, 10.1038/nature21058, 2017.

Wang, Y., Wu, L., Hu, W., Li, W., Shi, Z., Harrison, R. M., and Fu, P.: Stable iron isotopic composition of atmospheric aerosols: An overview, NPJ Clim. Atmos. Sci., 5, 75, 10.1038/s41612-022-00299-7, 2022.

Wei, T., Dong, Z., Zong, C., Liu, X., Kang, S., Yan, Y., and Ren, J.: Global-scale constraints on the origins of aerosol iron using stable iron isotopes: A review, Earth-Sci. Rev., 258, 104943, 10.1016/j.earscirev.2024.104943, 2024.

Weyer, S. and Schwieters, J.: High precision Fe isotope measurements with high mass resolution MC-ICPMS, Int. J. Mass Spectrom., 226, 355-368, 10.1016/s1387-3806(03)00078-2, 2003.

Wu, D., Zheng, H., Li, Q., Wang, S., Zhao, B., Jin, L., Lyu, R., Li, S., Liu, Y., Chen, X., Zhang, F., Wu, Q., Liu, T., Jiang, J., Wang, L., Li, X., Chen, J., and Hao, J.: Achieving health-oriented air pollution control

https://doi.org/10.5194/egusphere-2026-3780
Preprint. Discussion started: 14 July 2026

662 requires integrating unequal toxicities of industrial particles, Nat. Commun., 14, 6491, 10.1038/s41467-
663 023-42089-6, 2023.
664 Zhang, Y., Li, R., Bunnell, Z. B., Chen, Y., Zhu, G., Ma, J., Zhang, G., Conway, T. M., and Tang, M.: A
665 critical review of the use of iron isotopes in atmospheric aerosol research, Atmos. Chem. Phys., 25,
666 11067-11086, 10.5194/acp-25-11067-2025, 2025.
667 Zhao, X. M., Cao, H. H., Mi, X., Evans, N. J., Qi, Y. H., Huang, F., and Zhang, H. F.: Combined iron and
668 magnesium isotope geochemistry of pyroxenite xenoliths from Hannuoba, North China Craton:
669 implications for mantle metasomatism, Contrib. Mineral. Petrol., 172, 40, 10.1007/s00410-017-1356-y,
670 2017.
671 Zhu, G. H., Ma, J. L., Wei, G. J., and An, Y. J.: A novel procedure for separating iron from geological
672 materials for isotopic analysis using MC-ICP-MS, J. Anal. At. Spectrom., 35, 873-877,
673 10.1039/c9ja00446g, 2020.
674 Zuo, P., Huang, Y., Liu, P., Zhang, J., Yang, H., Liu, L., Bi, J., Lu, D., Zhang, Q., Liu, Q., and Jiang, G.:
675 Stable Iron Isotopic Signature Reveals Multiple Sources of Magnetic Particulate Matter in the 2021
676 Beijing Sandstorms, Environ. Sci. Technol. Lett., 9, 299-305, 10.1021/acs.estlett.2c00144, 2022.
677